



JOINT INSTITUTE FOR NUCLEAR RESEARCH
Dzhelepov Laboratory of nuclear problems

FINAL REPORT ON THE START PROGRAMME

*“Radiation Protection and the Safety of
Radiation Source”*

Supervisor

Prof.Dr.S. Abdelshakour

Students

Hayam Mohamed Elzeiny Abdelfattah Abdelgawad
Beni-Suef university, Egypt

Participation period

July 17 – September 3, 2022

Dubna, 2022

1. Introduction

All humans are exposed to ionizing radiation in one way or another, from natural or artificial sources, and consequently pose a possible risk to human health. That is why the use of radiation and radioactive material must be assessed and controlled by means of the application of standards of safety. Dose limits are recommendations based on our knowledge of the detrimental impact of excessive radiation on biological materials. The International Commission on Radiological Protection (ICRP) recommends the separation of the exposures into three categories: occupational, medical, and the general public. A dose higher than 100mSv as a single exposure event or accumulated over one year causes a significant risk of cancer and an increased probability of tissue reactions^{1,2}. Therefore, one of the most important factors for those who work with or around radiation is to be aware of the levels of radiation around them and this can be mainly achieved by using variant types of radiation detectors. Having the basic knowledge of the different types of detectors and understanding how they operate can help to find the best appropriate detector for the required task and also can maximize the benefits of operating that detector^{3,4,5}.

Radiation detectors of a wide variety are used for detecting, measuring, characterizing, and classifying radiation emissions. The three main functions that characterize a radiation detector are (1) a radiation absorber, (2) an observable phenomenon from the interaction, and (3) a method to measure the observable. Various types of radiation detectors are used depending on the energy and the type of particle to be counted and the purpose of the measurement. The 3 main types of radiation detectors are the gas-filled detectors, the scintillators-based and the semiconductor detectors⁶. Here in our project, we focused on using CdTe, BGO, NaI, and pixel detectors for detection of different types of radiation particles such as alpha, beta, gamma, X-ray and we studied their different characteristics and parameters.

2. Methods

During this course, we used different types of detectors such as; CdTe , BGO, NaI and Pixel. Every detector has its characteristics. Therefore, here we studied the following properties:

- The calibration curve of detectors.
- The resolution of detectors.
- Detection of unknown source.
- Calculation the registration efficiency spectrum.
- Calculation the Attenuation coefficient of different shields.
- Detection of α -particles range in the air by pixel detector and theoretically by SRIM software.

So, each method is explained in details in the following result section.

3. Results

3.1. X-123 CdTe detector

The X-123CdTe is used for X-Ray and Gamma-Ray detection. It is small with area (25 mm^2), and thickness (1 mm), low power (2.5 Watts), high performance, and simple to operate.

- Its components: the CdTe detector, a preamplifier, a DP5 digital pulse processor (DPP) and MCA, and a PC5 power supply.



The X-123CdTe and Mini-X on the MP1 mounting plate.

Figure.1. X-123CdTe Experimental Set-up.

Task(1): Detection Energy calibration curve of the CdTe detector:

Calibration curve is the result of the relation between channel number and its corresponding energy (Kev).

To detect the calibration curve for CdTe detector:

- We used a radioactive source of known energy spectrum such as Co57 .
- Detect the corresponding energy of each channel number from the background spectrum of the detector (Fig.2a) with its energy spectrum (Fig.2b) from Co57 source.
- Plot the calibration curve by linear fitting to obtain the calibration equation (Figure 3).

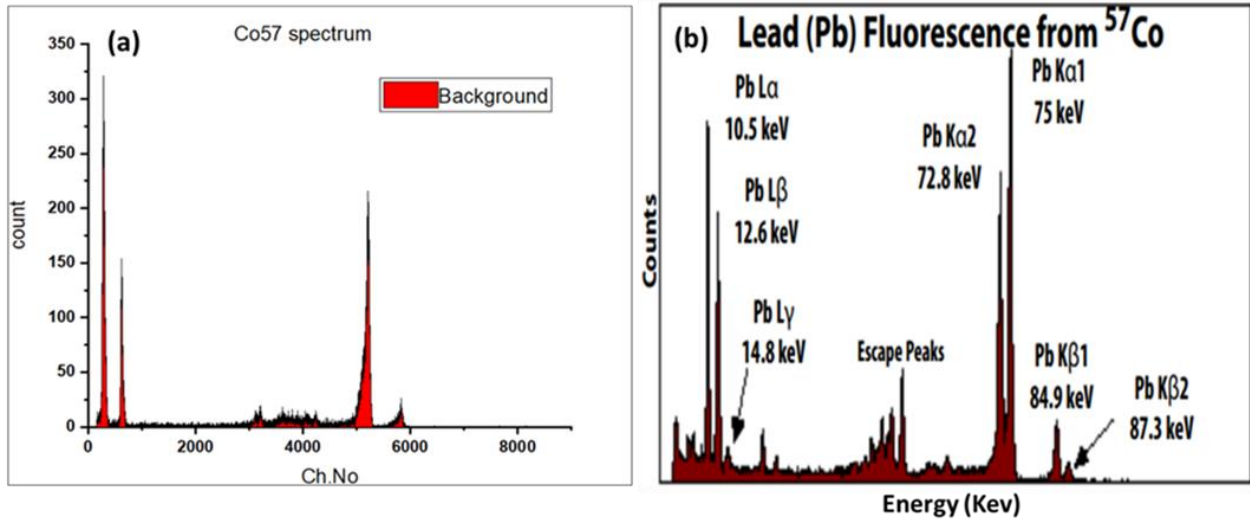


Figure.2. (a) The background spectrum of the CdTe detector, and (b) its known energy spectrum from Co⁵⁷ source.

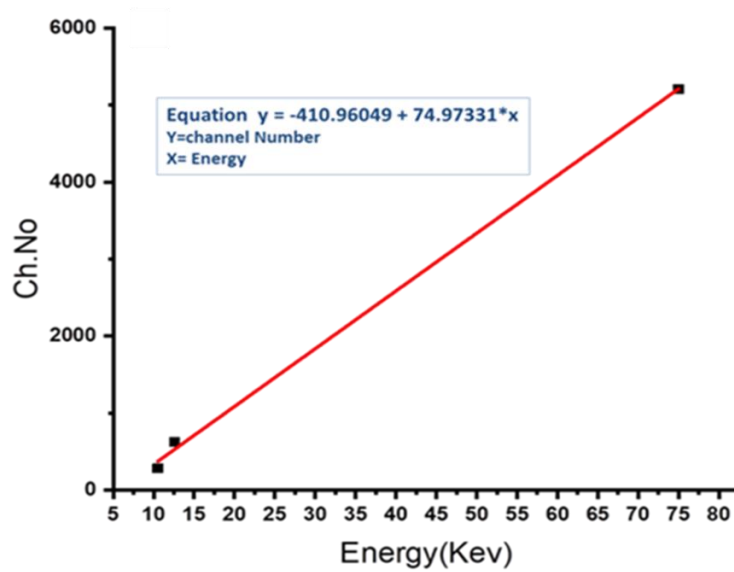


Figure.3. Energy calibration curve for CdTe detector by using Co⁵⁷.

Task(2): Detection the resolution of CdTe detector:

Resolution of the detector is its ability to accurately determine the energy of the incoming radiation and separate between adjacent energy peaks.

It can be calculated from the following equation:

$$R = \frac{\sigma}{Mean} \times 2.35 \times 100$$

- Resolution is the plot between energy and count by applying Gaussian fitting to the peaks of a given data of Co⁵⁷ spectrum (Figure.4).

- This plot depends on the previous calibration equation $y = -410.96049 + 74.97331*x$, we can calculate the Energy (Kev).

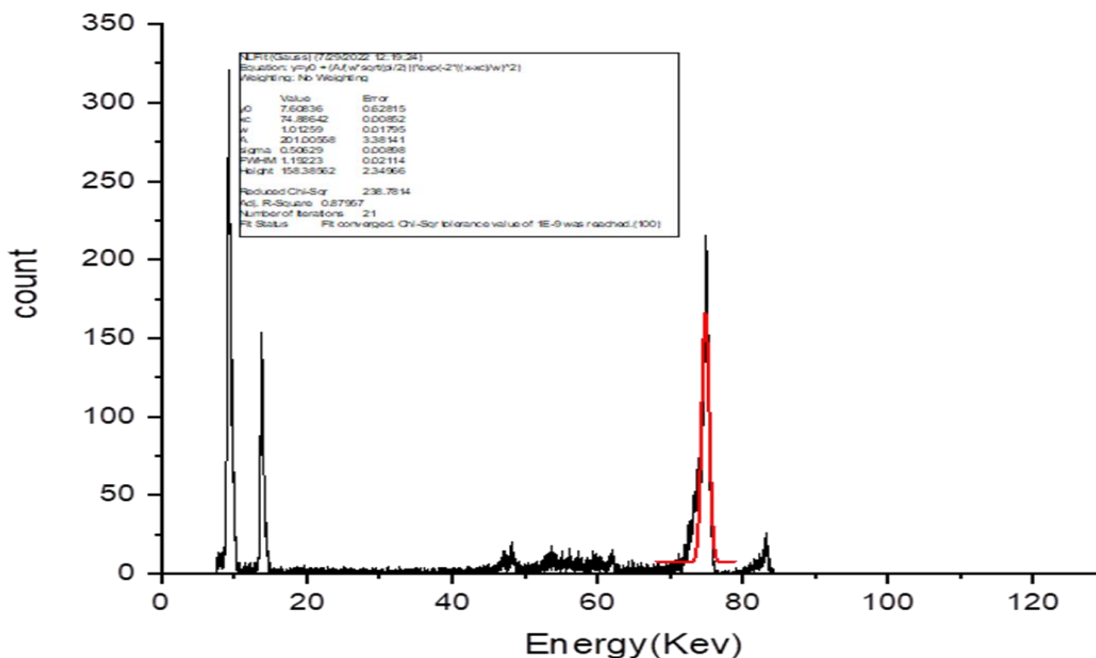


Figure.4. Resolution of CdTe detector by using Co^{57} source.

From this figure by knowing the values of sigma and mean, R can be calculated:

$$R = \frac{0.50629}{74.88642} \times 2.35 \times 100 = 1.58878\% \text{ at Energy 75 keV}$$

Task(3): Calculation the real spectrum of CdTe detector:

The detector count Efficiency is related to the amount of radiation emitted from radiation source to the measured amount in the detector.

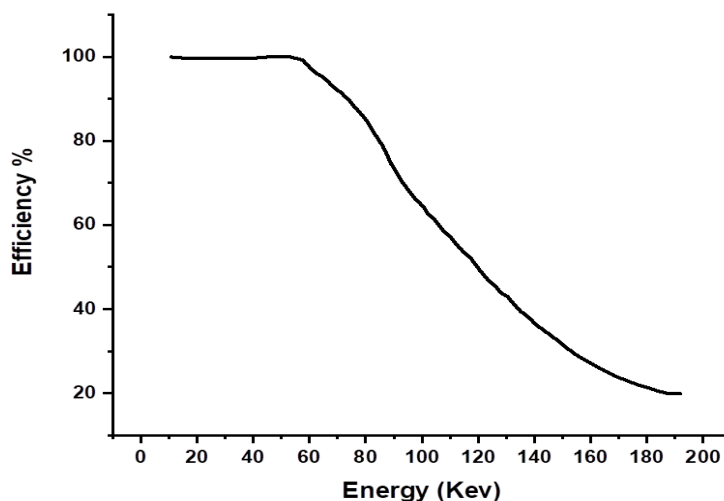


Figure.5. The registration Efficiency of CdTe detector at thickness 1mm of CdTe sensor.

Task(1): Detection the resolution of BGO detector

- To detect the resolution of BGO detector, we use different applied voltage ranging from 1200 to 2000 V.
- Get the value of sigma and Mean by Gaussian fitting using ROOT to at different applied voltages.
- Resolution is plotted against voltage by using Co^{60} as a source of radiation.

Table (1): Showing resolution calculations of Co^{60} radiation energy detected with BGO crystal detector.

Applied voltage (V)	Sigma	Mean	R%
1200	0.46001	1.60318	67.42966
1300	0.25006	1.36426	43.0738
1400	0.295	1.92404	36.03083
1500	0.46529	2.984	36.64275
1600	0.59087	4.43087	31.33807
1700	0.7822	6.09198	30.17372
1900	1.23041	10.6745	27.08758
2000	1.54712	13.6163	26.70132

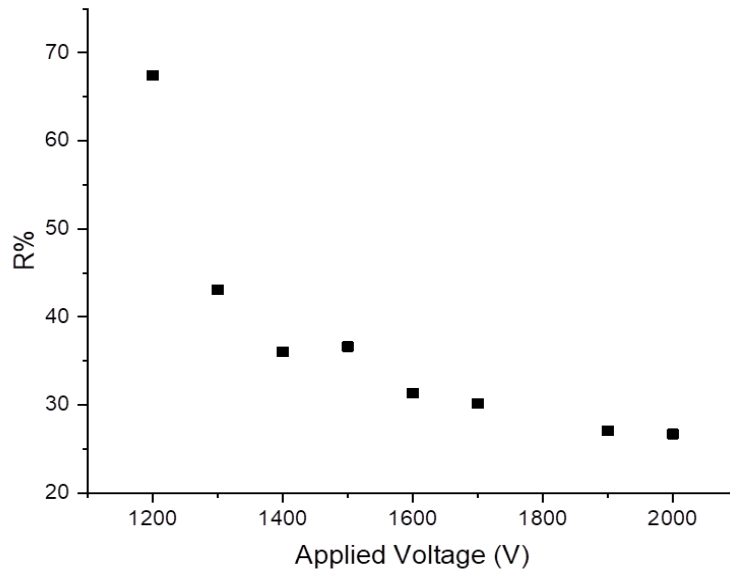


Figure.8. The Resolution Curve of the BGO detector.

We noticed that as the applied voltage increases, the resolution of the detector gets better, and it is the highest value at 2000V.

Task(2): Energy calibration of BGO detector

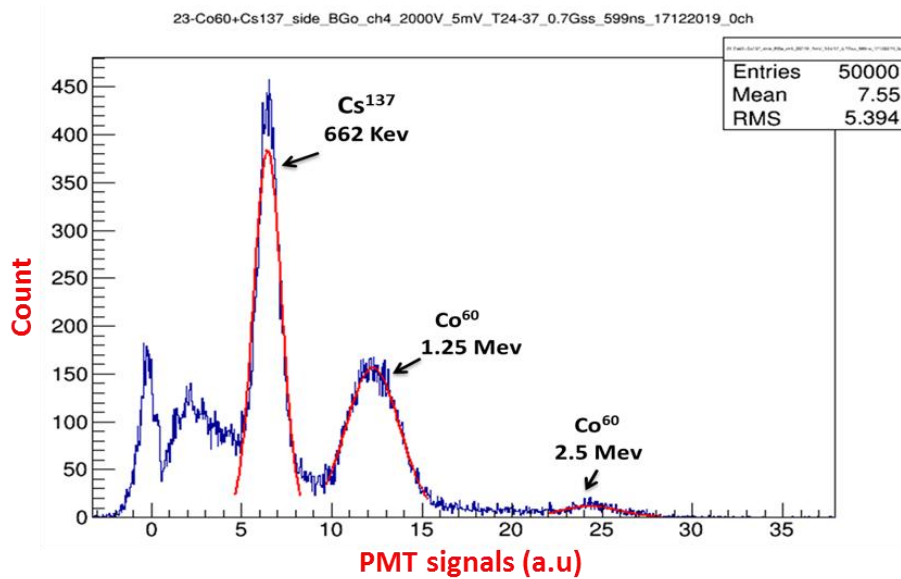


Figure.9. Energy spectrum of Cs^{137} and Co^{60} by BGO detector.

From the above graph, we can draw the calibration energy curve for BGO by linear fitting.

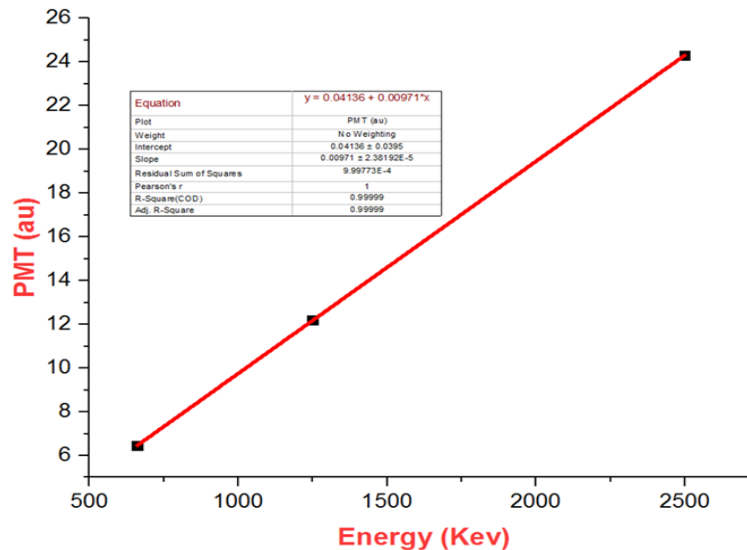


Figure.10. Calibration Energy curve for BGO detector.

Task(3): Identification of unknown sources

- Getting the spectrum of unknown source
- Making GAUSSIAN FIT and find Mean for each peak
- Determining energy peak of unknown source by using calibration equation:

$$y = 0.04136 + 0.00971 \cdot x$$

Where; $y =$ PMT signal (a.u), $X =$ Energy of unknown isotope source.

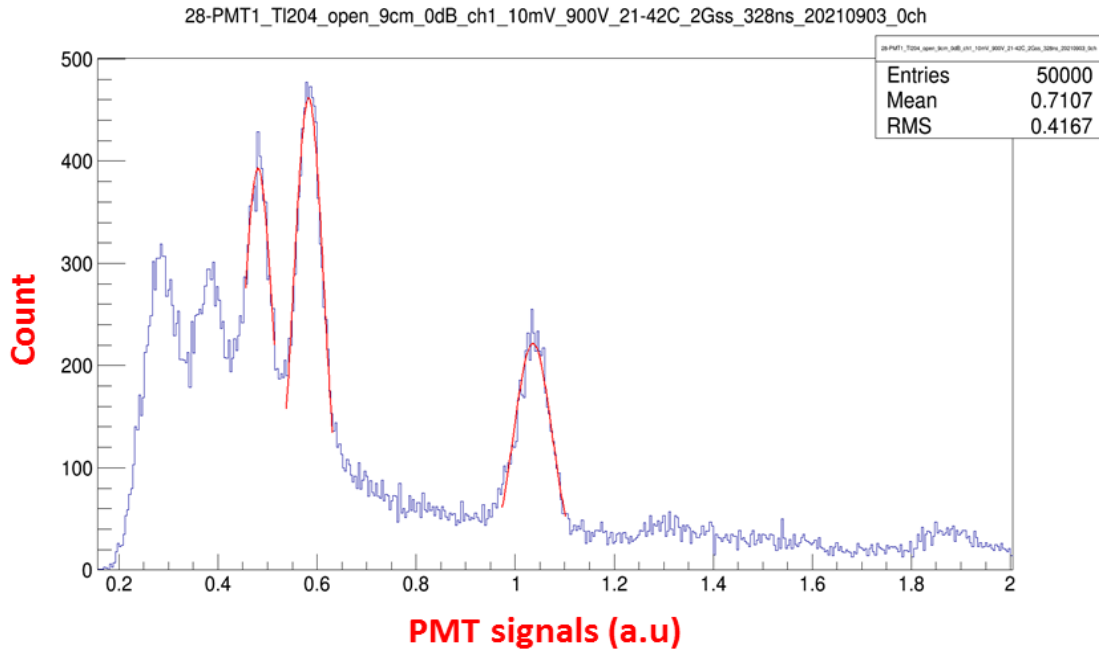


Figure.11. The spectrum of unknown source.

Table (2): Detection the unknown isotopes by their calculated energy peak.

PMT signal	Energy(Kev)	Unknown isotope
0.48117	45.29403	Sm
0.583	55.79156	Hf
1.03577	102.41092	¹⁵⁵ Tb

Task(4): The Attenuation coefficient:

- Attenuation coefficient describes the fraction of a beam that is absorbed or scattered per unit thickness of the absorber.
- It is calculated using the following equation:

$$I_x = I_0 e^{-\mu x}$$

Where I_x is the intensity at depth of x cm, I_0 is the original intensity, and μ is the linear attenuation coefficient.

Attenuation coefficient for Aluminum and copper

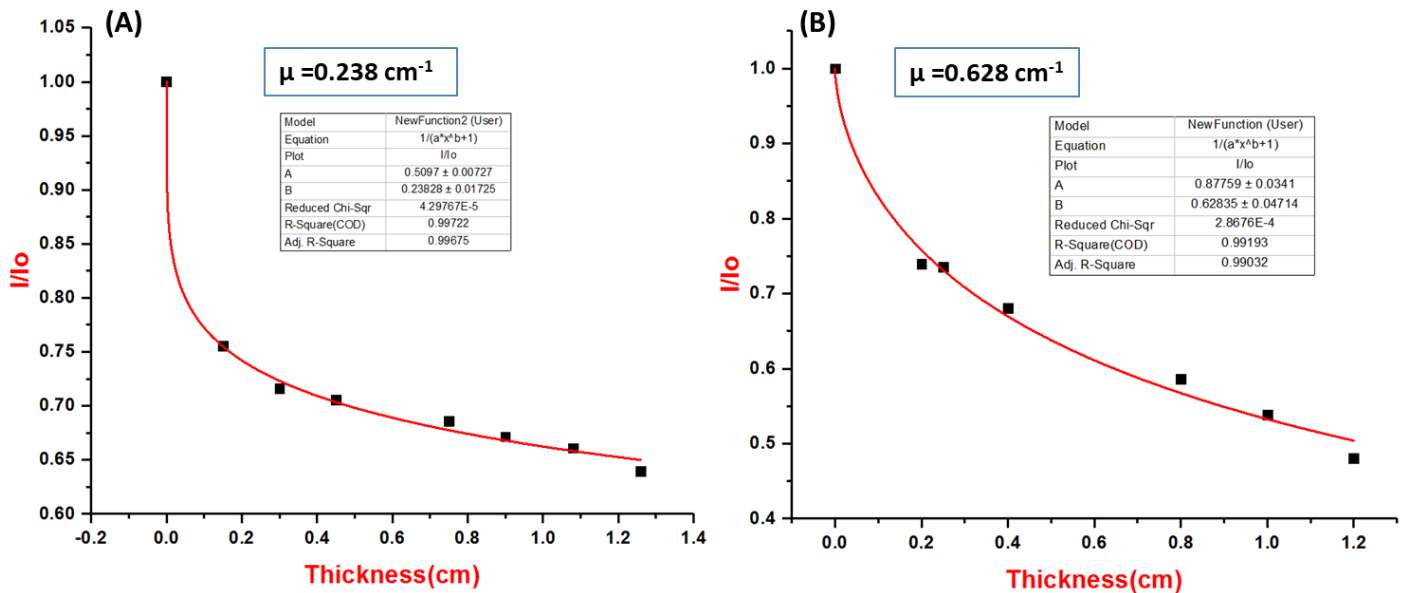


Figure.12. Attenuation coefficient for (A)Al, and (B)Cu using Cs^{137} at E662 Kev by BGO detector.

From the previous figures A and B; linear attenuation coefficient of Cu is higher than linear attenuation coefficient of Al as it increases with increasing atomic number and increasing physical density of the absorbing material.

3.2.2. NaI detector

It has the same principle of BGO detector in detection of radiation.

Task(1): Detection the resolution of NaI detector

$$R = \frac{\sigma}{Mean} \times 2.35 \times 100$$

Applied Voltage(V)	Sigma	Mean	R%
900	0.6081	23.6799	6.03477
1000	1.01022	40.6248	5.84376
1100	1.55464	65.7823	5.55378
1200	2.01024	98.7595	4.7834
1300	2.60369	137.477	4.45069

Table (2): Showing resolution calculations of Co^{60} radiation energy detected with NaI crystal detector.

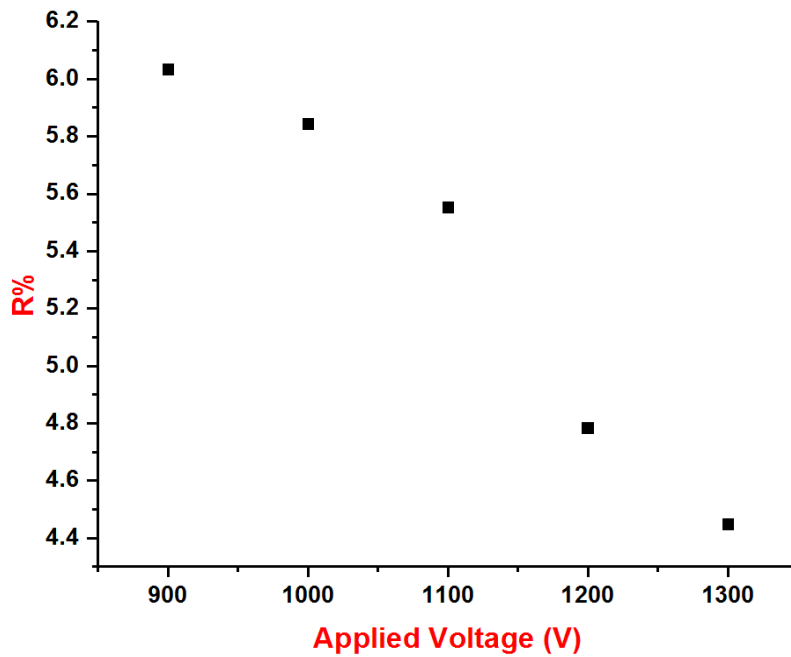


Figure.13. The resolution Curve of NaI detector

Task(2): Energy calibration of NaI detector

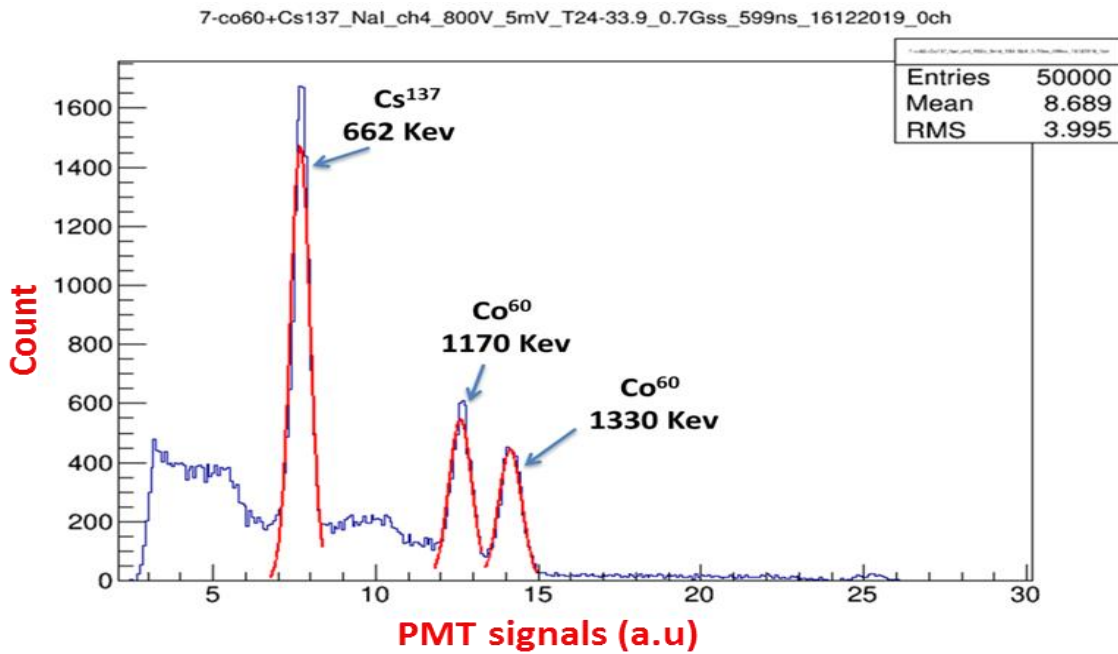


Figure.14. Energy spectrum of Cs¹³⁷ and Co⁶⁰ by NaI detector at 2000 V.

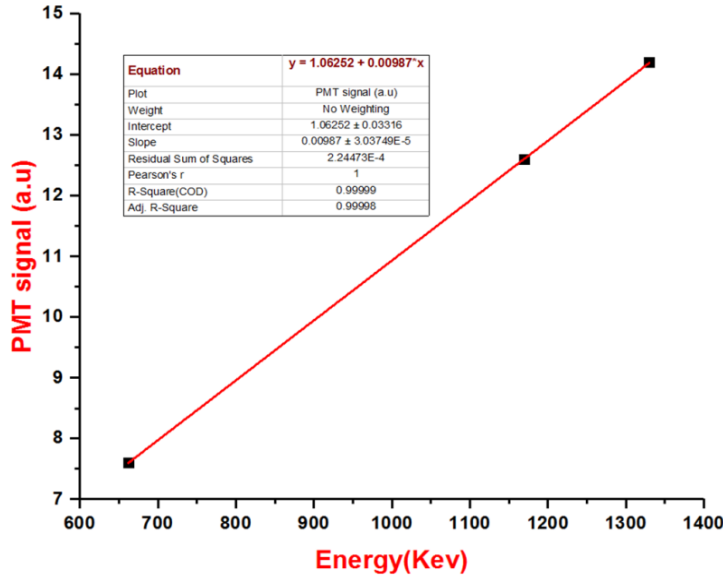


Figure.15. Calibration Energy curve for NaI detector.

Task(3): Identification of unknown sources

From the previous equation of calibration, we can detect the unknown sources by GAUSSIAN FIT.

Equation of calibration:

$$y = 1.06252 + 0.00987 \cdot x$$

where, y = PMT signal A.U, x = Energy of unknown source

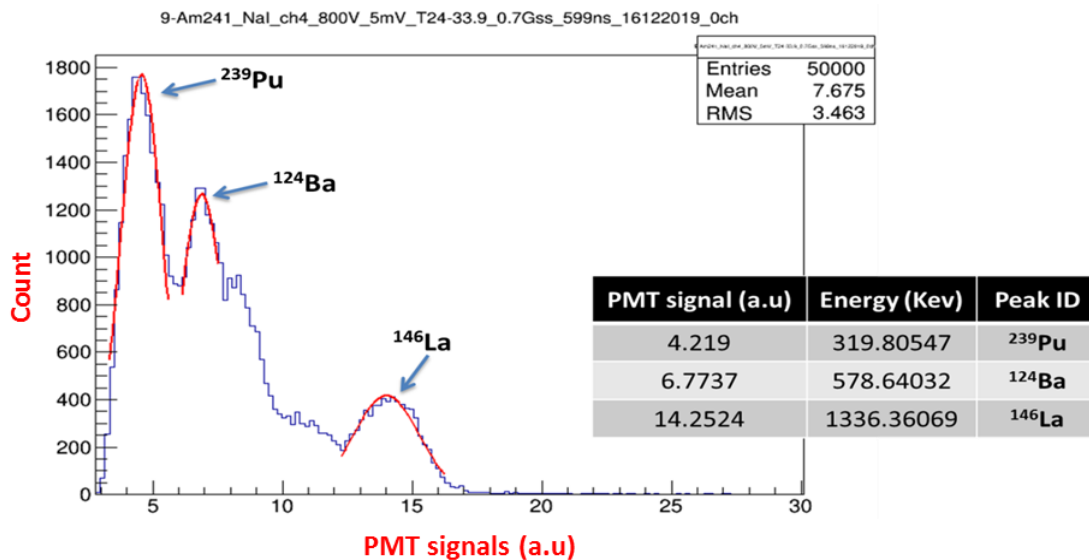


Figure.16. Energy spectrum for unknown sources.

3.3. Pixel detector:

- It is an advanced detector like a digital camera.
- It consists of: (1) Sensor (Si), (2) Chip Channels, (3) USB.

- It is characterized with its high resolution.
- It detects the radiation of α , β , γ particles using Am^{241} , Uranium ($\text{U}^{238} + \text{U}^{235}$), Thorium.



Figure.17. MEDPIX MX-10 Detector complete set-up.

MX-10 Detector: It is a pixel semiconductor ionizing radiation detector.

Its main elements: a 14×14 mm semiconductor silicon sensor

- it is covered with solid metallization “Aluminum layer”
- 256×256 square pixels(65.536) with a size of $55 \mu\text{m}$

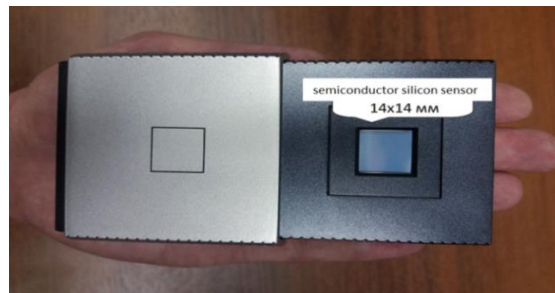


Figure.18. MX-10 Detector.

Task(1): Visualization of α , β , γ particles:

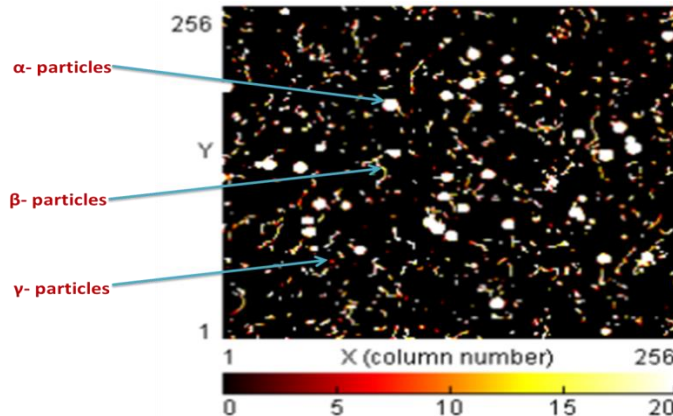


Figure.19. α , β , γ particles by Pixel detector using Thorium radiation source.

Task (2):The relation between α -particles count and distance.

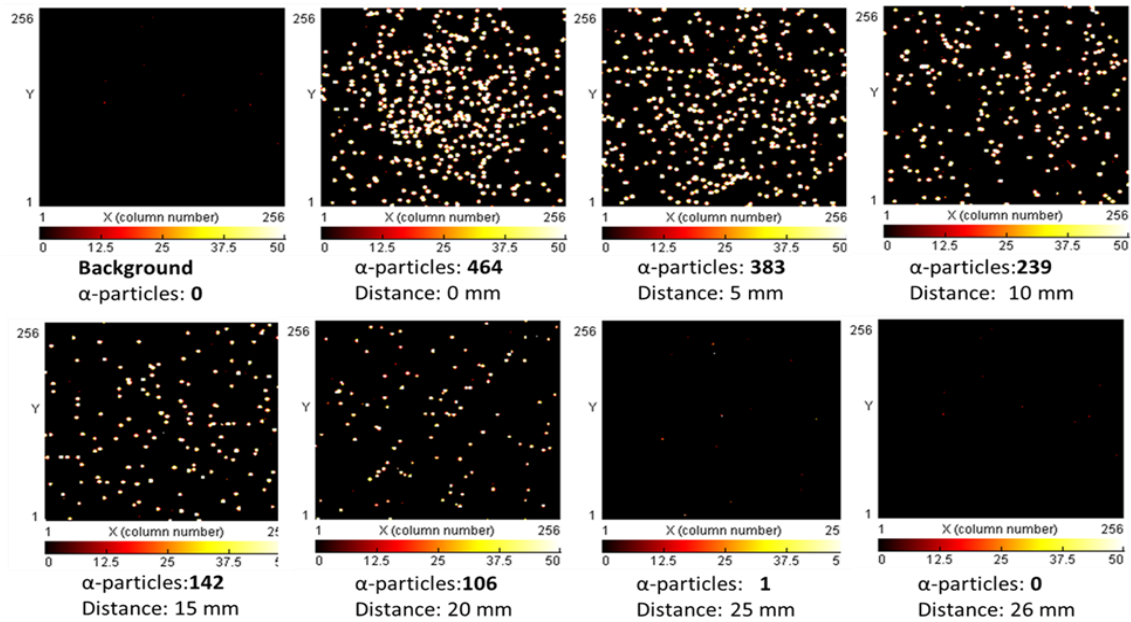


Figure.20. The relation of α -particles count from Am^{241} source with the distance of it from the pixel detector at 50 V(applied volt) and constant time intervals (3mins).

From figure.20. The count number of α -particles decreases dramatically with increasing the distance of Am^{241} source from the detector till reaches to 0 at 26mm (max range).

Task(3): Detection the range of α -particles in the air theoretically:

By using Monte Carlo Simulation “SRIM software”.

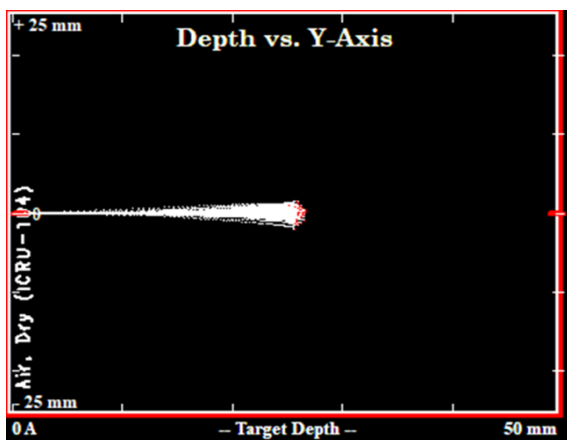


Figure.21. Depth of α -particles in the dry air.

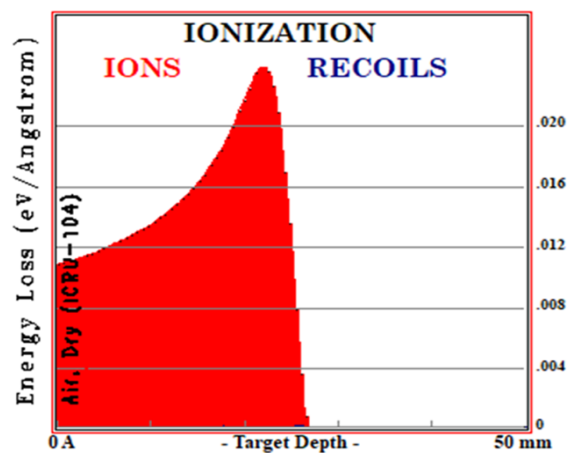


Figure.22. Ionization.

Where: Target: Dry air - Source: Am^{241} - Ions: $^4He^2$ - Energy of He = 4 Mev - Target Density = 1.204 g/cm^3

From figure.21. α -particles are completely stopped at 26 mm deep in dry air (Max calculated range) and this is the same value of alpha particles range in the experiment.

Task(4): The relation of energy loss with target depth

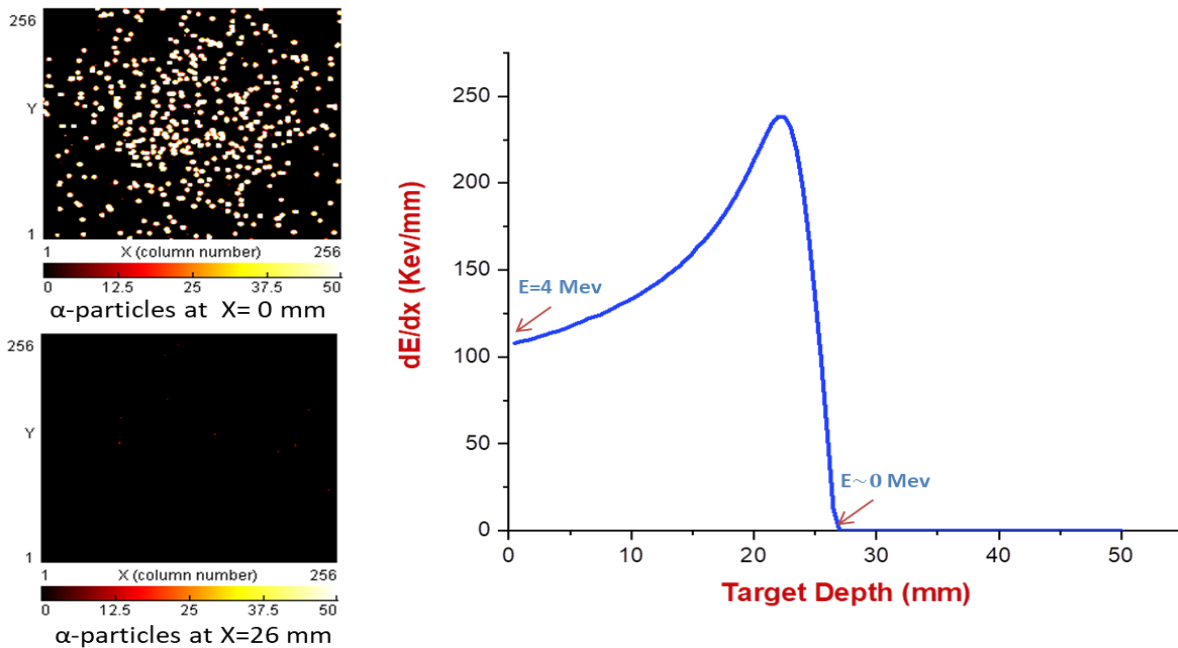


Figure.23.the relation of energy loss of α - particles (4 Mev) with target depth.

Task(5): Energy loss of alpha particles in the air at different depth.

By using Am^{241} source with $E= 4000$ Kev

X (mm)	0	5	10	15	20	25	26
E (Kev)	4000	505.5	1130	1855.5	2769.7	3844.7	3940.8

4. Conclusion

During this project, I studied the basics knowledge of radiation safety and protection from different radiation sources and how to detect them by different instruments. I acquired the essential practical skills, tools, and softwares for analyzing the spectrum obtaining from CdTe, Scintillation detectors (BGO, NaI), and I have done many tasks for studying the different characteristics of these detectors; evaluation Energy calibration of these detectors by using known spectrum of radioactive sources, calculation their resolution, identifying the unknown sources based on the spectrum from known radioactive ones, detection the attenuation coefficient for different shielding material by BGO detector. In addition, using pixel detectors for determining α -particles range in air, and energy loss of α -particles in the air and comparing them with the values obtained from Monto carlo simulation via SRIM software.

5. Acknowledgements

First of all, I wish to offer my heartfelt thanks to my supervisor **Prof. Dr Said AbouElazm** for allowing me to be a part of such an interesting project, and I want to express my deep gratitude for his explanation and constant guidance throughout the period. I would like to express my special thanks to **Mr.K.papenkov** for giving me a chance to do my experiment in his laboratory, and to **Mr.Dmitry Kharchenko** for providing me with his computer during that time. I am also grateful for having a chance to meet wonderful people like **Mr.Igor Liashko** who took of his time out to help and guide me and to share his knowledge with me about detectors.

I have to extend my supreme gratitude to **the Joint Institute for Nuclear Research (JINR) Centre** for providing such kind of opportunity for students to broaden their background knowledge and discover more areas of research interests under prominent supervisors. I would like to thank also START program coordinators **Ms.Julia Rybachuk**, and **Ms.Elena Karpova** for organizing this great session and their effort to make sure that the program achieves its desired goals.

6. References

- 1- Cerrito, Lucio. "Radiation and detectors." Cambridge University (2017).
- 2- Morgan, William F., and William J. Bair. "Issues in low dose radiation biology: the controversy continues. A perspective." *Radiation research* 179.5 (2013): 501-510.
- 3- Attix, Frank Herbert. *Introduction to radiological physics and radiation dosimetry*. John Wiley & Sons, 2008.
- 4- Cember, Herman, and Thomas E. Johnson. *Introduction to health physics*. NNRA Library, 2009.
- 5- "Introduction To Radiation Detectors". Mirion.Com, <https://www.mirion.com/learning-center/radiation-detector-types/introduction-to-radiation-detectors>.
- 6- Shultis, J. Kenneth, and Richard E. Faw. *Fundamentals of nuclear science and engineering*. CRC press, 2016.